NANO EXPRESS

Synthesis and Growth Mechanism of Ni Nanotubes and Nanowires

Xiaoru Li · Yiqian Wang · Guojun Song · Zhi Peng ·
Yongming Yu · Xilin She · Jianjiang Li

Abstract Highly ordered Ni nanotube and nanowire arrays were fabricated via electrodeposition. The Ni microstructures and the process of the formation were investigated using conventional and high-resolution transmission electron microscope. Herein, we demonstrated the systematic fabrication of Ni nanotube and nanowire arrays and proposed an original growth mechanism. With the different deposition time, nanotubes or nanowires can be obtained. Tubular nanostructures can be obtained at short time, while nanowires take longer time to form. This formation mechanism is applicable to design and synthesize other metal nanostructures and even compound nanostuctures via template-based electrodeposition.

Keywords Nanotubes · Nanowires · Growth mechanism · Electrodeposition

Introduction

Nanostructures have received comprehensive attention owing to their novel optical, electrical, catalytic and magnetic properties and their potential applications in nanoscale electronic, sensing, mechanical and magnetic devices [1, 2], and information storage systems [3–6].

X. Li · G. Song (✉) · Z. Peng · Y. Yu · X. She · J. Li
Institute of Polymer Materials, Qingdao University, No. 308
Ningxia Road, Qingdao 266071, China
e-mail: songguojunqdu@126.com

Y. Wang
Laboratory of Advanced Fiber Materials and Modern Textile,
The Growing Base for State Key Laboratory, Qingdao
University, No. 308 Ningxia Road, Qingdao 266071,
People's Republic of China

Among various synthetic processes, template synthesis has been proved to be a versatile and simple approach for the preparation of many nanostructures, such as conductive polymers, metals, semiconductors, carbon and other materials [7–10]. Among these materials, metal nanostructures have been the focus of extensive research activities due to their unusual properties [11]. Many groups have focused on the magnetic properties of nickel (Ni) nanotubes and/or nanowires [12–15], because of their small magnetocrystalline anisotropy energy and potential application in devices. Some groups have studied the formation mechanism of the Ni nanostructures [16–21], but the growth mechanism is still unclear so far. Therefore, a complete understanding of the growth mechanism needs intense investigation. This has aroused our interest to explore the growth mechanism of Ni nanotubes and nanowires.

In our work, we not only report the successful fabrication of ordered Ni nanotube and nanowire arrays using anodic aluminum oxide (AAO) templates by changing electrodeposition conditions, but also propose a growth mechanism for Ni nanotubes and nanowires. The proposed growth mechanism for Ni nanotubes and nanowires in our work is different from others reported before and is easier for the readers to understand. The obtained Ni nanotubes are more likely to enable us to fix metals or semiconductors in order to achieve novel nanocomposites with unique physical properties, and the Ni nanowire arrays might have potential applications in the magnetic–electric devices.

Experimental Section

Nanotubes and nanowires were synthesized using template-directed electrochemical deposition, an approach pioneered

by Martin [7, 8]. In general, AAO films are formed by the electrochemical oxidation of aluminum. Depending on the type of anodization process and growth regime used, aluminum oxide membranes can be fabricated to contain nanopores with a wide range of diameters, lengths and interpore distances. To facilitate nanowire fabrication, commercially available aluminum oxide membranes, Whatman Anodisc 25, were used, with a nominal pore diameter ranging from 150 to 300 nm and depths ranging from 50 to 60 μm.

The side of the AAO membrane was sputtered with a layer of Au as a work electrode. In a tri-electrode electrochemical system, the Ni nanostructure arrays were produced in the template pores from a solution of 0.8 mol/L $NiSO_4 \cdot 6H_2O$ + 0.5 mol/L H_3BO_3 + 0.3 mol/L KCl by direct current electrodeposition. The electrodeposition was carried out using platinum as an anode and a calomel electrode as a reference electrode. Finally, the nanowire arrays were revealed by the removal of AAO in a 3 mol/L sodium hydroxide solution. Three samples were prepared under different electrodeposition conditions. They were labeled as sample 1 (applied voltage: −0.8 V, deposition time: 20 min, corresponding current: 0.03–0.11 mA), sample 2 (−0.8 V, 40 min, 0.03–0.19 mA) and sample 3 (−0.8 V, 60 min, 0.04–0.26 mA).

The morphology of the Ni nanostructure arrays was investigated using a JEOL JSM-6390LV SEM. The structure and microstructure of the Ni nanotubes and nanowires were investigated using a JEOL JEM-2000EX TEM. The specimen for TEM observation was prepared by evaporating a drop (5 μL) of the nanostructure dispersion onto a carbon-film-coated copper grid. The growth process of Ni nanotubes and nanowires was investigated using high-resolution transmission electron microscope (HRTEM).

Results and Discussion

With different deposition time, Fig. 1a–f show clearly the top-view and side-view images of Ni nanostructures with different deposition time. Figure 1a shows a typical SEM image of highly ordered nanotube arrays with a deposition time of 20 min obtained after the removal of AAO in aqueous NaOH, illustrating clear open ends. As deposition time increases, nanowires were formed. Figure 1c and e show the morphologies of nanowires formed after a deposition time of 40 and 60 min respectively. From Fig. 1c, e, the top views of the nanowires, it can be clearly seen that the Ni nanowires have solid ends. The length of the Ni nanostructures increases with the electrodeposition times. Figure 1b, d, f present side views of Ni nanotubes and nanowires corresponding to Fig. 1a, c, e, respectively. It is clear that the length of the Ni nanowires shown in

Fig. 1f is the longest, about 20 μm, and in Fig. 1b is the shortest, about 3 μm.

It can be seen from Fig. 1 that there is a length distribution for the nanotubes and nanowires in each sample. This is due to the difference of barrier layer thickness at each pore and also due to the hydrogen evolution caused by water-splitting reaction [22]. Ni^{2+} ions are reduced during the electrodeposition by the electrons tunneled through the barrier layer. However, the barrier layer at each pore could be branched differently during the thinning process of the barrier layer, resulting in different energy barriers for tunneling because of different barrier layer thickness [23]. The number of tunneled electrons through an insulating layer decreases exponentially with the thickness of the insulating layer according to Bethe's equation [24]. Consequently, the rate of deposition becomes different at each pore.

The formation process of Ni nanowires was investigated using TEM. Figure 2 presents typical TEM images of these three samples. Figure 2a shows that some nanostructures have a characteristic of half wire and half tube. It is believed that the wire end is the starting point. As time increases, Ni nanotubes and nanowires coexist in the same template under the same experimental conditions, as shown in Fig. 2b. Figure 2c shows that whereas most nanostructures are Ni nanowires, a small amount of nanostructures is nanotubes. It can be seen from Fig. 2c that nanowires are not very uniform: one end is a little thicker than the other end, and some nanowires have branches. It depends on the quality of the commercial AAO templates, as shown in the SEM image of AAO pores (Fig. 2d).

From the TEM results, we conclude that the formation process of Ni nanowires begins with the formation of Ni nanotubes. Nanotubes were formed at first, and then Ni nanoparticles of the electrode stacked randomly in the tubes, until nanowires were formed. The formation process is revealed vividly in Fig. 2a. With the increase in deposition time, nanotubes disappear gradually, and the amount of nanowires increases further. However, nanotubes still exist despite of the increased deposition time, because Ni^{2+} ions concentration in the margin region of the templates is low and can not be supplemented from the whole solution in time. So, Ni nanoparticles are not enough to fill the Ni nanotubes in time; therefore, Ni nanotubes still exist in the margin regions of the templates.

The formation process of the Ni nanostructures was further investigated using HRTEM. Figure 3a shows that a small amount of nanoparticles is randomly arranged in the inner surface of the Ni nanotubes. However, the amount of nanoparticles increases with the deposition time. It can be seen clearly that nanoparticles (in Fig. 3b)

Fig. 1 Typical SEM images of Ni nanotube and nanowire arrays obtained under different conditions: (**a**), (**c**) and (**e**) are top views of samples 1, 2 and 3 respectively; (**b**), (**d**) and (**f**) are side views of the samples 1, 2 and 3 respectively
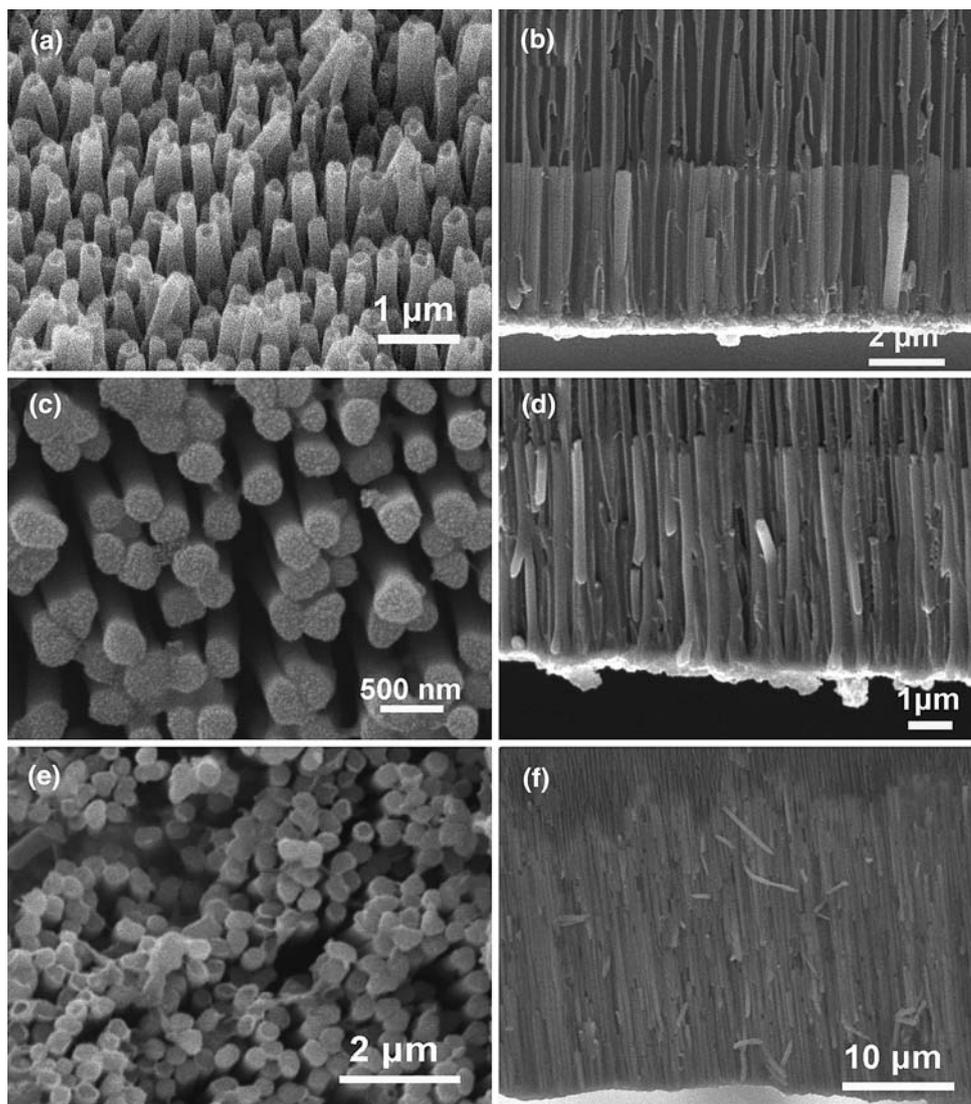

are much more than those in Fig. 3a. A certain amount of Ni nanoparticles joined together to form Ni nanotubes. As the deposition time increases, more and more Ni nanoparticles join together to form a wire, as can be seen in Fig. 3c. From Fig. 3c, it can be seen that the nanowire is formed by many nanograins with different crystallographic orientations.

Based on our experimental results, deposition time is a critical condition to produce nanotubes or nanowires. However, applied current density (E field) affected the formation of nanotubes and nanowires. Figure 4 illustrates schematic diagrams of the electrodeposition process for Ni nanotubes and nanowires. Figure 4a provides a clear understanding of the growth mechanism of Ni nanotubes. The junction between the electrode surface and the bottom edge of the template pore serves as a preferential site for the deposition of metal ions, because the inner walls of the

nanochannels have surface absorption energy [25, 26]. At the beginning, Ni ions move toward the electrode and receive electrons to become atoms. A certain amount of atoms can aggregate together to form Ni nanoparticles, which are absorbed onto the surface of the inner walls of the nanochannels. When the surface absorption energy is stronger than the E field, Ni nanoparticles will be preferentially distributed on the surface of the inner walls of the nanochannels, and tubular nanostructures are obtained as mentioned earlier.

Figure 4b shows vividly the formation process of the nanowires. When Ni nanotubes are formed, the surface absorption energy of nanochannels decreases accordingly. When the E field is preferential, Ni nanoparticles begin to stack inside the tubes from the electrode surface until the nanotubes are completely filled, and nanowires are obtained.

Fig. 2 TEM images of Ni nanowires and nanotubes: (**a**) sample 1, (**b**) sample 2, (**c**) sample 3 and (**d**) SEM image of AAO pores
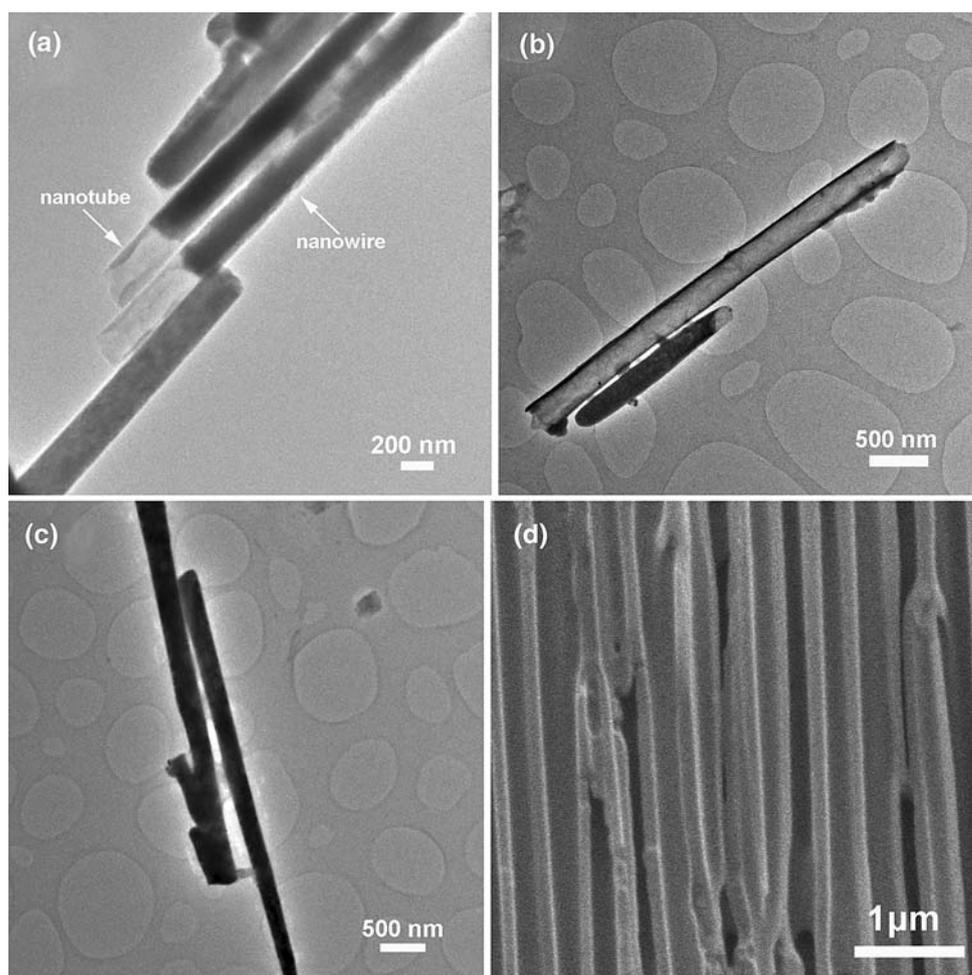
In summary, nanoparticles stack inside the tubes to form nanowires when the E field reached a certain value. We have termed this growth mechanism brick-stacked wirelike growth (BSWG). Cao et al. [20] have proposed a current-directed tubular growth (CDTG) mechanism. They believed that metal nanotubes can be obtained at $v_\parallel$ (growth rate parallel to current direction) » $v_\perp$ (growth rate perpendicular to current direction), while nanowires can be obtained at $v_\parallel \approx v_\perp$. However, we think that it is difficult to define the competitive rates.

It is well known that Ni is a magnetic material with very small magnetocrystalline anisotropy energy [12]. The crystallographic orientations of these nanoparticles are different, so the shape anisotropy of these nanoparticles is also different. The adjacent nanoparticles will repel each other, resulting in Ni nanoparticles being randomly arranged and the grains having different crystallographic orientations, as shown in Fig. 3c.

Our results fully demonstrate that magnetic materials can form nanotubes and nanowires under appropriate synthesis conditions. We believe that the BSWG mechanism can be applied to synthesize other magnetic metal nanostructures. Controlling the synthesis conditions, other metal nanostructures can be deposited in magnetic nanotubes to form novel nanocomposite materials.

Conclusion

In summary, highly ordered Ni nanotubes and nanowires have been fabricated by DC electrodeposition in the pores of AAO templates under the deposition voltage of −0.8 V. Ni nanotubes were obtained when the deposition time was less than 20 min, and the corresponding current was 0.03–0.11 mA, while Ni nanowire arrays were obtained when the deposition time was more than 40 min and when the current was more than 0.19 mA. Systematic HRTEM investigations demonstrate the formation process of Ni nanostructures, and the growth mechanism for Ni nanotubes and nanowires has also been explored. We believe that the BSWG mechanism can be applied for other magnetic nanostructures; especially, such metal

Fig. 3 HRTEM images of Ni nanowires and nanotubes for samples under different conditions: (**a**) sample 1, (**b**) sample 2 and (**c**) sample 3
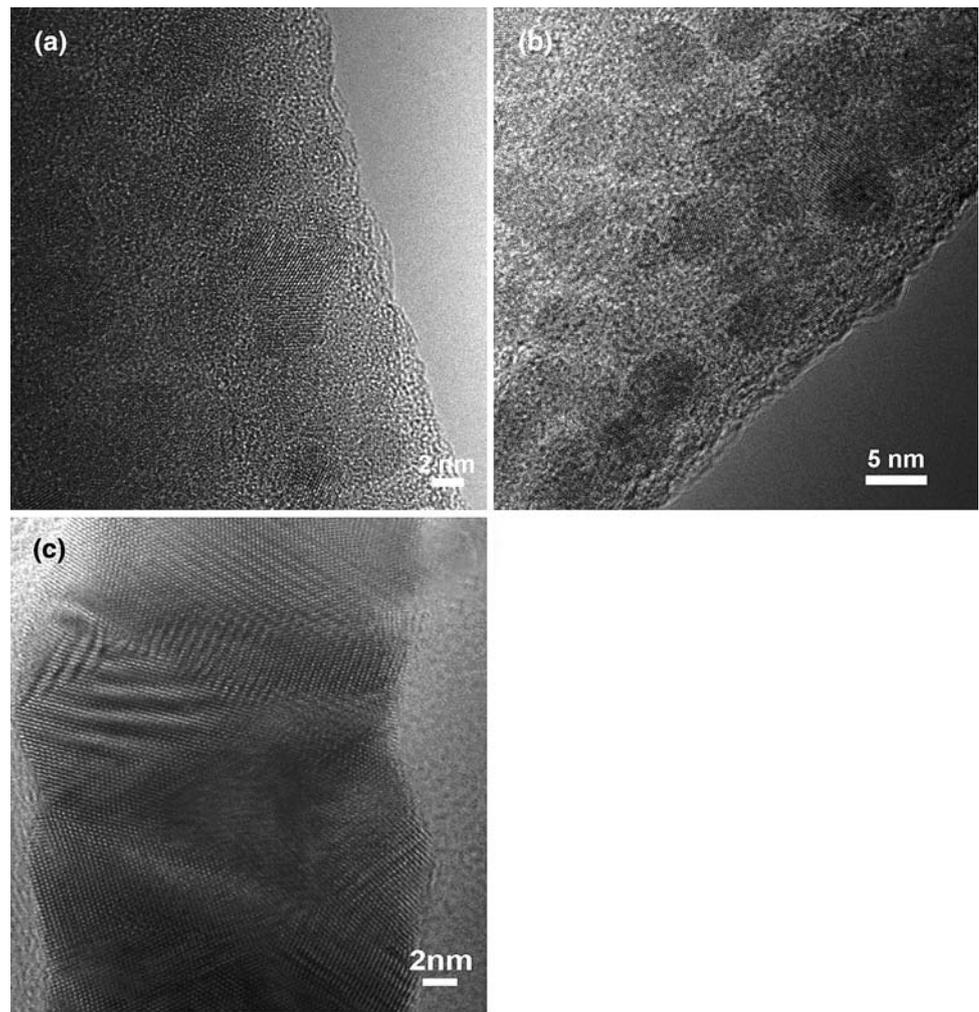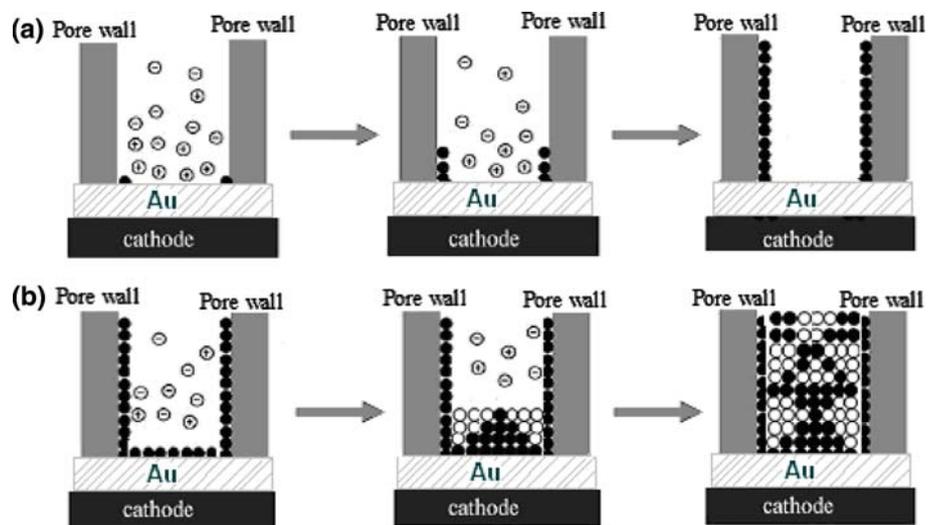

Fig. 4 a Schematic diagram of the growth process of nanotubes; **b** Schematic diagram of the growth process of nanowires (the white and black balls showing different crystallographic orientations)

nanotubes with open ends have a variety of promising applications, such as porous electrodes filled with ferromagnetic and nonmagnetic metals to fabricate magnetic multilayer nanostructure, or other materials to prepare novel nanocomposite materials with special magnetic, optical or electrical properties.

References

1. N.I. Kovtyukhova, T.E. Mallouk, Chem. Eur. J. **8**, 4354 (2002). doi:10.1002/1521-3765(20021004)8:19<4354::AID-CHEM4354>3.0.CO;2-1

2. F. Patolsky, G. Zheng, O. Hayden, M. Lakadamyali, X. Zhuang, C.M. Lieber, Proc. Natl. Acad. Sci. U.S.A. **104**, 14017 (2004). doi:10.1073/pnas.0406159101

3. M.S. Gudiksen, L.J. Lauhon, J.F. Wang, D.C. Smith, C.M. Lieber, Nature **415**, 617 (2002). doi:10.1038/415617a

4. Y. Cui, Q.Q. Wei, H.K. Park, C.M. Lieber, Science **293**, 1289 (2001). doi:10.1126/science.1062711

5. T. Thurn-Albrecht, J. Schotter, C.A. Kästle, N. Emley, T. Shibauchi, L. Krusin-Elbaum, K. Guarini, C.T. Black, M.T. Tuominen, T.P. Russell, Science **290**, 2126 (2000). doi:10.1126/science.290.5499.2126

6. H.P. Liang, Y.Q. Guo, J.S. Hu, C.F. Zhu, L.J. Wan, C.L. Bai, Inorg. Chem. **44**, 3013 (2005). doi:10.1021/ic0500917

7. C.R. Martin, Science **266**, 1961 (1994). doi:10.1126/science.266.5193.1961

8. C.R. Martin, Chem. Mater. **8**, 1739 (1996). doi:10.1021/cm960166s

9. A. Huczko, Appl. Phys. A **70**, 365 (2000). doi:10.1007/s003390051050

10. K. Peng, Z. Huang, J. Zhu, Adv. Mater. **16**, 73 (2004). doi:10.1002/adma.200306185

11. K.R. Pirota, D. Navas, M. Hernandez-Velez, K. Nielsch, M. Vazquez, J. Alloy Compd. **369**, 18 (2004). doi:10.1016/j.jallcom.2003.09.040

12. F. Tian, J. Zhu, D. Wei, J. Phys. Chem. C **111**, 12669 (2007). doi:10.1021/jp0737294

13. M. Hangarter Carlos, V. Myung Nosang, Chem. Mater. **17**, 1320 (2005). doi:10.1021/cm047955r

14. M.A. Mousa, J. Imran, Alloys Compd. **455**, 17 (2008). doi:10.1016/j.jallcom.2007.01.051

15. J.B. Shi, Y.C. Chen, C.W. Lee, Y.T. Lin, C. Wu, C. Chen, J. Mater. Lett. **62**, 15 (2008). doi:10.1016/j.matlet.2007.04.060

16. H. Pan, B.H. Liu, J.B. Yi, C. Poh, S.H. Lim, J. Ding, Y.P. Feng, C.H.A. Huan, J.Y. Lin, J. Phys. Chem. B **109**, 3094 (2005). doi:10.1021/jp0451997

17. C.G. Jin, W.F. Liu, C. Jia, X.Q. Xiang, W.L. Cai, L.Z. Yao, X.G. Li, J. Cryst. Growth **258**, 337 (2003). doi:10.1016/S0022-0248(03)01542-2

18. D.J. Sellmyer, M. Zheng, R. Skomski, J. Phys.: Condens. Matter **13**, R433 (2001)

19. F. Tian, J. Chen, J. Zhu, J. Apply, Phys **103**, 013901 (2008)

20. H.Q. Cao, L.D. Wang, Y. Qiu, Q.Z. Wu, G.Z. Wang, L. Zhang, X.W. Liu, ChemPhysChem **7**, 1500 (2006). doi:10.1002/cphc.200500690

21. Q.T. Wang, G.Z. Wang, X.H. Han, X.P. Wang, J.G. Hou, J. Phys. Chem. B **109**, 23326 (2005). doi:10.1021/jp530202

22. S.K. Hwang, S.H. Jeong, O.J. Lee, K.H. Lee, Microelectron. Eng. **77**, 2 (2005). doi:10.1016/j.mee.2004.07.069

23. Y.C. Sui, B.Z. Cui, L. Mart′nez, R. Perez, D.J. Sellmyer, Thin Solid Films **406**, 64 (2002). doi:10.1016/S0040-6090(01)01769-2

24. E.E. Polymeropoulos, J. Appl. Phys. **48**, 2404 (1977). doi:10.1063/1.324002

25. M. Lahav, T. Sehayek, A. Vaskevich, I. Rubinstein, Angew. Chem. **115**, 5734 (2003). doi:10.1002/ange.200352216

26. M. Lahav, T. Sehayek, A. Vaskevich, I. Rubinstein, Angew. Chem. Int. Ed. Engl. **42**, 5576 (2003). doi:10.1002/anie.200352216